Hierarchichal Current Control Design For Electromagnetic Aircraft Launching System

A.Monti, K. Patel, D. Patterson, D. Kovuri and R. Dougal,
Department of Electrical Engineering
University of South Carolina, Swearingen Center
Columbia, SC 29208 USA

ACKNOWLEDGMENTS

This work was supported by the US Office of Naval Research (ONR) under grant N00014-02-1-0623.

ABSTRACT

This paper describes an approach to hierarchichal modular control for an electromagnetic aircraft launching system for the aircraft carrier of the future. The purposes are to analyze the possibility of improving the control performance using efficient evaluation of switching conditions, and to explore the different options for the basic control design and the way in which these designs will be tested using the Virtual Test Bed (VTB) Software. After the descripition of the application of deadbeat control, in conjunction with predictive algorithms, to the Control, back electro-magnetic force (emf) generated by FEA (Finite Element Analysis) is discussed. The non-ideal shape of the back emf produces torque ripple in the control. It is shown that this ripple can be easily compensated for by the new control scheme proposed. The new control scheme is tested under two different conditions: two-phase control (or DC brushless) and three-phase control (AC brushless).

Introduction

Modern ship designs are increasingly oriented towards the use of electricity to distribute, control, and deliver energy for all on-board needs. In some significant cases, including traction, adoption in military applications is rather slow, because of the comparatively low achievable power, energy and torque, per unit volume and per unit mass, of electro-mechanical energy conversion systems. However, the benefits of controllability, robustness, reliability, damage management, operational availability, reduced manning, etc. are undeniable. Hence there is a high level of interest in electromagnetic aircraft launching systems for aircraft carriers. The goal is to design and test an electromagnetic system to replace steam catapults as the energy source for launching aircraft off Navy carriers. This paper will concentrate on the control aspect of this kind of system. In the first section an introduction is given to the basic machine design for a linear motor dedicate to this kind of application. The second section discusses the modular control implemented in VTB. The third section focuses on the back emf analysis using FEA and on the problem of torque ripple. In the final section a new scheme is introduced to control a permanent magnet motor as a Brushless AC to compensate for this torque ripple. The simulation platform used for the project is the VTB Software [1]. Other details of the linear motor design project can be found in [2].

Basic Machine Format

In this research project, the majority of effort so far has been directed to a permanent magnet version of the machine. It consists of a stator, which is approximately 110 meters long and a shuttle that is 3 meters long. The schematic of stator and shuttle is shown in Fig. 1.

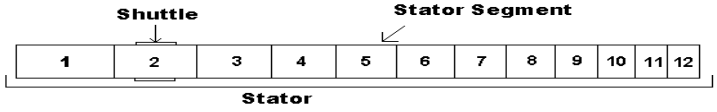

Fig. 1: EMALS stator and shuttle (not to scale)

The stator hosts a multiphase winding structure, while the magnets are located in the shuttle. The stator windings are organized in segments. The detailed machine design and power electronics switching matrix design can be found in [2].

Control Design

For an aircraft launching system the speed loop is not actually significant; the main concern is the current loop. Considering the final goal of the aircraft take-off, what we want to achieve is maximum constant acceleration for the first part and then a much higher deceleration after the take-off to stop the shuttle.

The control design will employ two controllers for the two H Bridge sets, to implement the logic to alternatively switch the sections controlled by the respective bridge set, which is shown in the figure below.

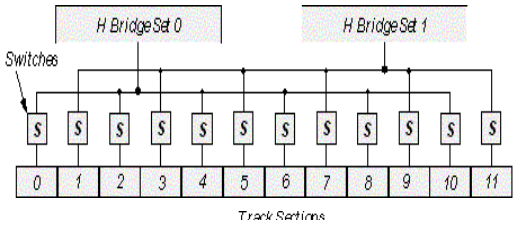

Fig. 2: Overall Switching Matrix

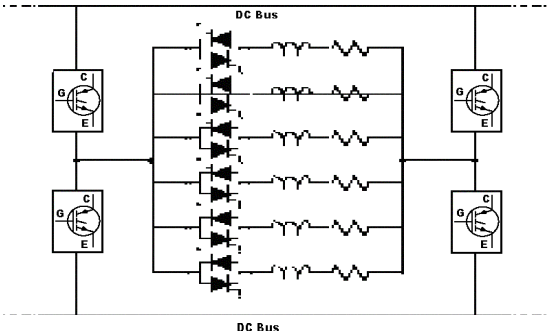

Fig. 3: The H-bridge, thyristor winding connection

One top-level controller will control these two controllers. Considering the high power involved in the design, we want to optimize the commutation frequency and the duty cycle. To achieve performance of the torque control, a fast current control scheme must be incorporated. Different options are currently under consideration and are part of a simulation activity performed within the VTB environment.

One possible approach is based on the deadbeat control in conjunction with predictive algorithms. A good combination of the two approaches can give important improvements in the control performance. We have the possibility of limiting the sampling rate and fixing the switching frequency to a constant value.

In any given sampling interval, we can bring the present sample value (at the beginning of the switching period) to the reference value at the end of the sampling time by defining a point at the interval t+ from the current sample value, such that the final sample value will be equal to the reference value, as shown in Fig. 4 below.

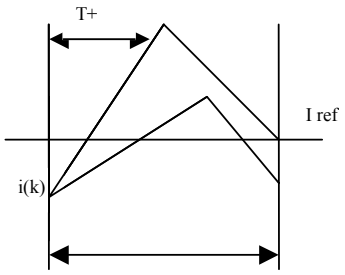

Fig. 4: The deadbeat control using t^+

Using the predictive variable structure control given by [3], we can find a value of t+ for the Permanent Magnet Brushless motors, which is shown below,

$$t^{+} = \frac{L\left(i_{REF} - e^{\frac{R}{L} T_c} \cdot i(k) \right) + k \cdot \omega \cdot T_s}{V_{dc}} \qquad (1)$$

The control uses the feedback values of current and speed to calculate the value of t^{+} for the next time step (eq. (1)), which is also graphically shown in Fig. 4. A detailed derivation can be found in [4]. The main drawback of this algorithm is the possibility of introducing biased ripple content. This will not allow for assurance of an accurate torque control; however, it can be easily pre-compensated as will be discussed in the section on torque ripple compensation.

The Simulation platform and modeling

Details of the simulation approach adopted in the project have been reported in [2]. In order to accommodate the requirements of the control design, the models have been ported to the new version of VTB [5]. VTB is a software environment that supports design, analysis and virtual prototyping of electrical circuits [6]. It has been developed at the Department of Electrical Engineering at the University of South Carolina. The VTB platform allows us to exploit the possibility of the Hierarchical modeling approach, which perfectly fits the modular structure of the linear motor.

Fig. 5 below shows the modular control structure in VTB that implements the torque control using the above algorithm. In the following experiment, 3 stator sections of increasing length were used.

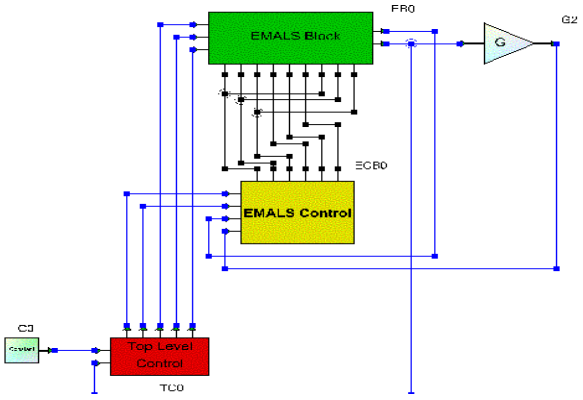

Fig. 5: Modular control experiment using deadbeat control

The top-level controller gets the length information for all the segments. The top block contains three stator segments of increasing lengths and one shuttle. It also contains the three power switch blocks for each stator section. The power switch gets the control signal from the bottom top-level controller. According to the given control signal, it enables or disables the current going to the corresponding stator section. An EMALS block is a hierarchical model and its schematic is shown in Fig. 6 below.

An EMALS Control block is hierarchical and a detailed schematic is shown in Fig. 7 below. It contains the main control block that implements the deadbeat control (left block) and also the inverter blocks (right DC/3AC block). The first inverter and control block supplies current to the odd segments, in this case the first and third segments, and the second inverter and control block supplies current to the even segments, in this case the second segment. The control block gets the reference current from the top-level controller based on shuttle position. This block assumes an ideal trapezoidal waveshape for the back emf and hence controls the motor as brushless DC motor.

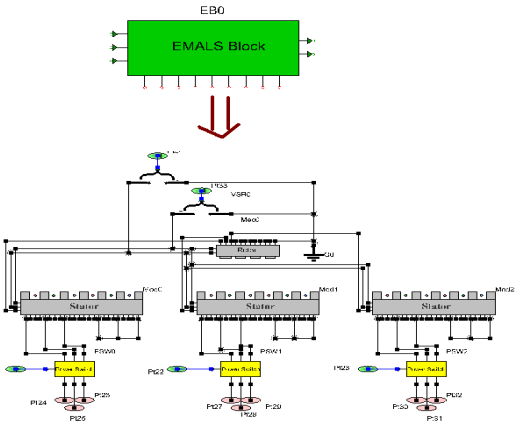

Fig. 6: Linear Motor Block (Hierarchical block)

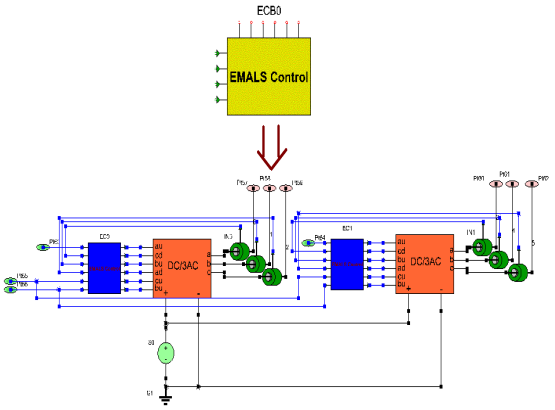

Fig. 7: EMALS Control Block (Hierarchical block)

The top-level controller gets the length information for all the segments as parameters. It also gets the shuttle position as feedback and uses this information to generate the reference current for an EMALS control blocks and the control signals for power switches.

The results are shown in Fig. 8 and Fig. 9. Fig. 8 shows the current flowing through the three segments. Once the shuttle leaves the corresponding segment, the current through that segment is switched to zero. Once the shuttle passes beyond the third segment the currents in all three segments are switched to zero. We can clearly see that as the shuttle slides on the segments, the currents through the segments are switched accordingly. Fig. 9 shows the classical trapezoidal waveform that appears only for those sections that are under the shuttle; we can clearly see the effects of acceleration.

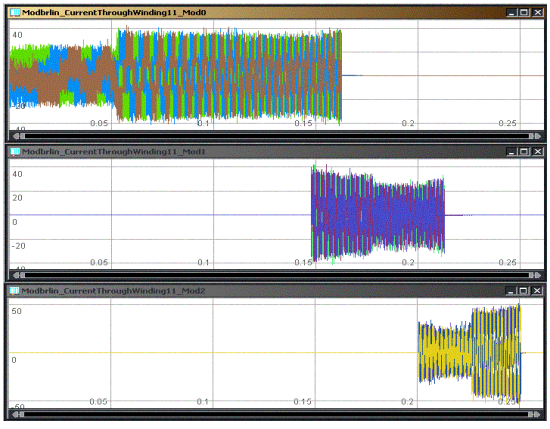

Fig. 8: 3-Phase Current Waveforms for three sequential segments as shuttle passes (square-wave thrust reference)

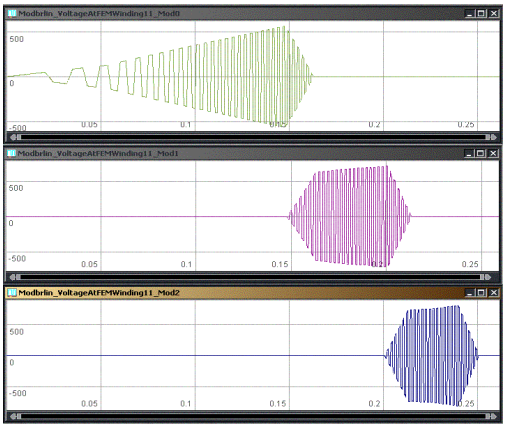

Fig. 9: Single phase back emf waveforms for three sequential segments as shuttle passes

Back EMF Analysis

Back EMF waveform generation by FEA using Ansoft

A model, shown in Fig. 10, to generate the back emf waveform for an EMALS model was designed in Ansoft's Maxwell 2D simulation tool. It consists of a 20-pole shuttle with 200 conductors. The materials assigned were copper for the conductor, steel for the stator and NdFeB for the magnets. The dimensions for the magnets are 120mm x 50mm and the conductors are 40mm x 20mm; air gap

is 5mm. The magnets are assigned north and south poles alternatively. The conductors are activated by a 3-phase supply with a peak current of 18000A.

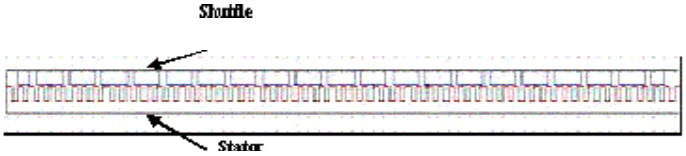

Fig. 10: Ansoft model for EMALS

The model setup is set to a refinement of up to 1% error and a current is applied in only one of the phases. The result of the simulation yields the value of force generated. This also includes the cogging torque (force with zero current) value and this is subtracted from the total force to get the required force waveform with respect to the degrees along the length of the stator. The force plot with the shuttle moving along the length of the stator with currents in one third of the conductors is as shown in Fig. 11 below.

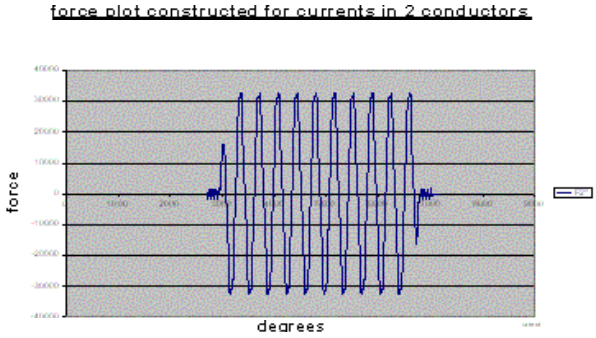

Fig. 11: Force plot for current in single phase

Because we know the value of current in one phase and the force (force plot fig c), from the equation F= BLi, we get the value of the constant BL. Applying this to E= BLv, where v is the velocity of the shuttle, we get the back emf wave. Following figures shows the force plot and back emf waveform for a single phase.

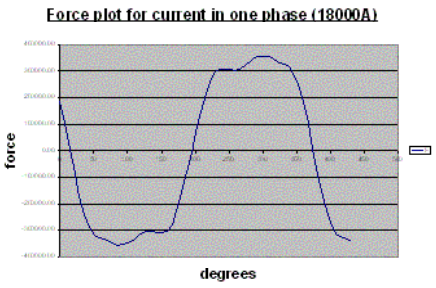

Fig. 12: Force plot for current in a single phase

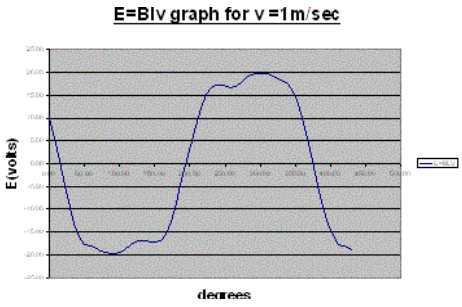

Fig. 13: Back emf waveform for current in a single Phase

Current is applied to only one phase and the shuttle is made to move over one pole pitch; the corresponding back emf and force plots are obtained as discussed above.

Interfacing results for Finite Element Analysis with VTB:

Software code was created in VTB through which this back emf data was exported from the Excel worksheet and read into the motor model. The following experiment was carried out in VTB to check the results. In this case, we have three stator section connected to the shuttle model. A force is applied

to the shuttle and then we measure the voltage across the open-circuited stator electrical windings. The VTB schematic for the experiment is shown in Fig. 14 below.

In this case we see the back emf waveform that appears only for those sections that are under the shuttle, which is shown in Fig. 15 below, and it is [illegible]cates the back emf obtained through FEA.

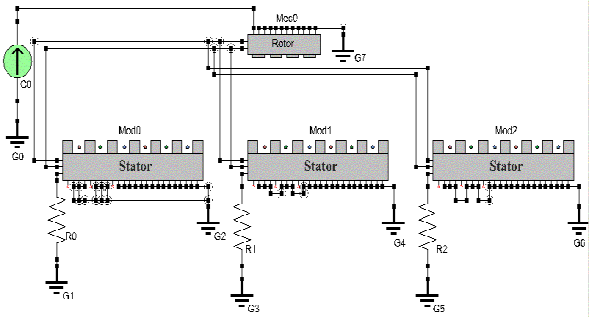

Fig. 14: VTB schematic to measure 3-phase back emf

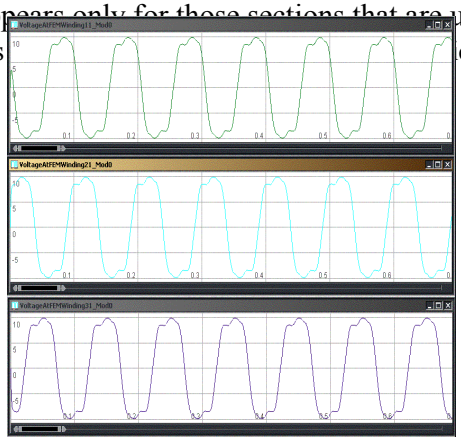

Fig. 15: 3-phase back emf waveforms obtained through FEA, represented in VTB

Torque ripple compensation

As we can see from Fig. 16 the back emf is non-ideal. It contains the even harmonics. This creates ripple in torque which can be seen from following results. The non-ideal back emf waveshape together with the brushless DC control of the motor, discussed in a previous section, generates a higher torque ripple in the control.

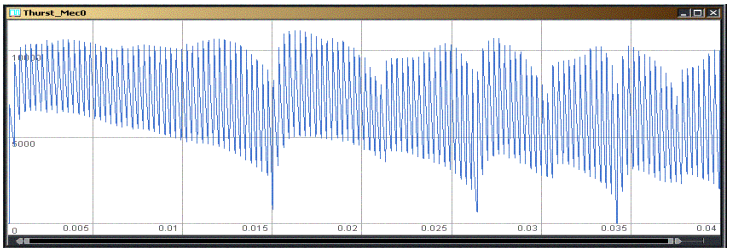

Fig. 16: Torque Ripple

Controlling the permanent magnet motor as a brushless DC motor always incurs the torque ripple problem. In brushless DC the commutation occurs at every 60^{o} and the torque ripple is generated in this period because the commutation requires a finite time due to the inductance and back emf [7],[8],[9]. If the machine has a non ideal trapezoidal back emf, the torque ripple appears even though rectangular currents are fed [10].

On the other hand fast current control in brushless AC motors incurs problems in high power applications [11]. At high power the switching frequency is limited due to the switching losses. Low switching frequency creates an increase in current distortions, machine losses, and torque ripple [12]. In brushless AC motors the back emf waveshape is assumed to be perfect sinusoidal.

In the following sections a new control approach is discussed for both brushless AC and DC motors that will result in reduced torque ripple in both cases and at the same time assuring fast current control. For torque ripple compensation, an algorithm is proposed in [13].It gives a unified approach to torque ripple limiting using an on line current compensation technique. By imposing the same torque variation it obtains the following expression for current variation.

$$\left|i_q(k+1)-i_q(k)\right| = \left\{\frac{a-b}{\varphi_q(k)}\right\}$$
$$a = \varphi_{md}\cdot\left[i_{q\_ref}(k+1)-i_{q\_ref}(k)\right] \quad (2)$$
$$b = \left[\varphi_q(k)-\varphi_q(k-1)\right]\cdot i_q(k)$$

A detailed derivation can be found in [13]. Using the above compensation function, the following hierarchical model was created in VTB.

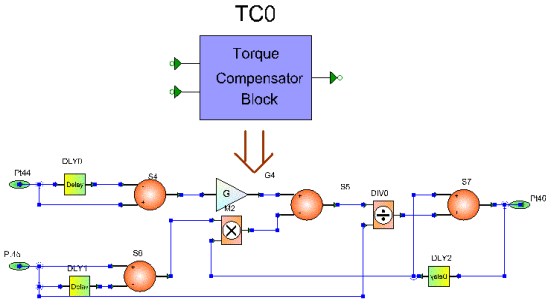

Fig. 17: The torque compensation block (Hierarchical Block)

This block requires the value of reference Current and the value of $\varphi_q(v) = \left.\frac{d\lambda}{dv}\right|_q$. The latter value can be easily evaluated for every motor. [14] Presents a mixed model for the motor in which no assumption has to be made about the waveshape of the back emf.

BLDC Control

In the case of BLDC, the value of $\varphi_q(v) = \left.\frac{d\lambda}{dv}\right|_q$ is found using the following assumption: We have values of $\left.\frac{d\lambda}{dv}\right|_{a,b,c}$ available through FEM analysis and we know that at any time positive current is flowing in one of the phases , negative current is flowing in the second phase and is zero in the third phase. With reference to that we can write the following equation;

$$\varphi_q(v) = \left.\frac{d\lambda}{dv}\right|_{i_1}\cdot i_1 + \left.\frac{d\lambda}{dv}\right|_{i_2}\cdot i_2 + \left.\frac{d\lambda}{dv}\right|_{i_3}\cdot i_3 = \left[\left.\frac{d\lambda}{dv}\right|_{i_1} - \left.\frac{d\lambda}{dv}\right|_{i_2}\right]\cdot i_1 \quad (3)$$

As $i_2 = -i_1, i_3 = 0$

A signal model in VTB was created which implements the logic mentioned above. The VTB schematic used to implement the BLDC control scheme is shown below,

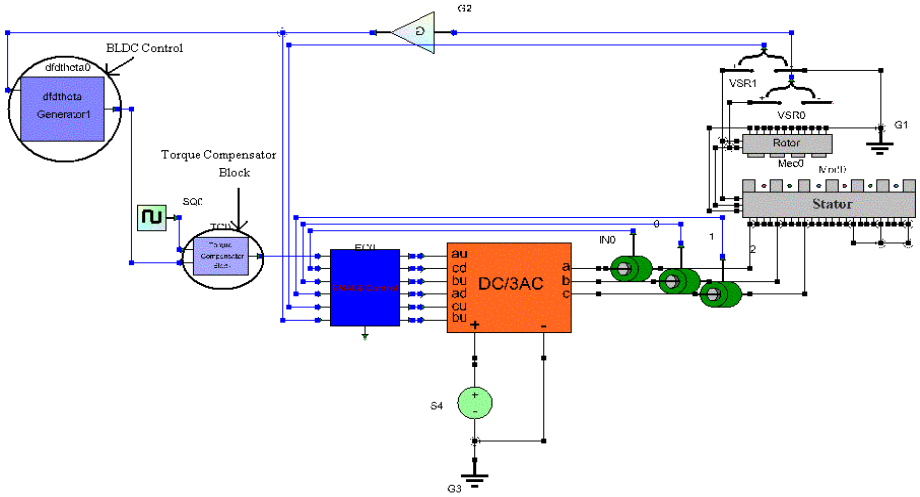

Fig. 18: The VTB schematic for BLDC control

In the following figure, t ent while the other graph shows the reference curre

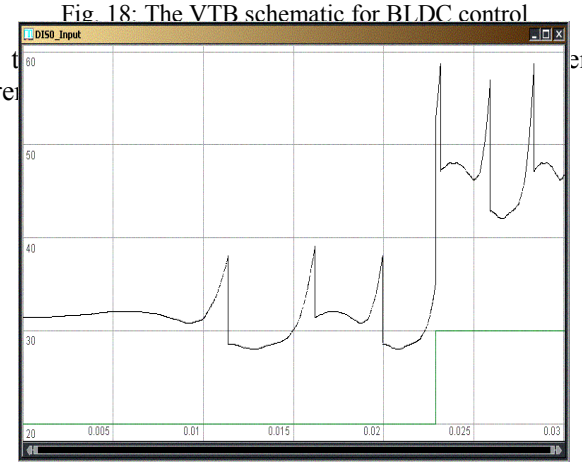

Fig. 19: Reference current generated by the torque compensator block

The 3-phase currents and the torque are shown below, and clearly the torque ripple is greatly reduced. The spikes in the torque ripple are created by the spikes in the reference current waveform, but the reatly reduced. Also the current control is shown to an

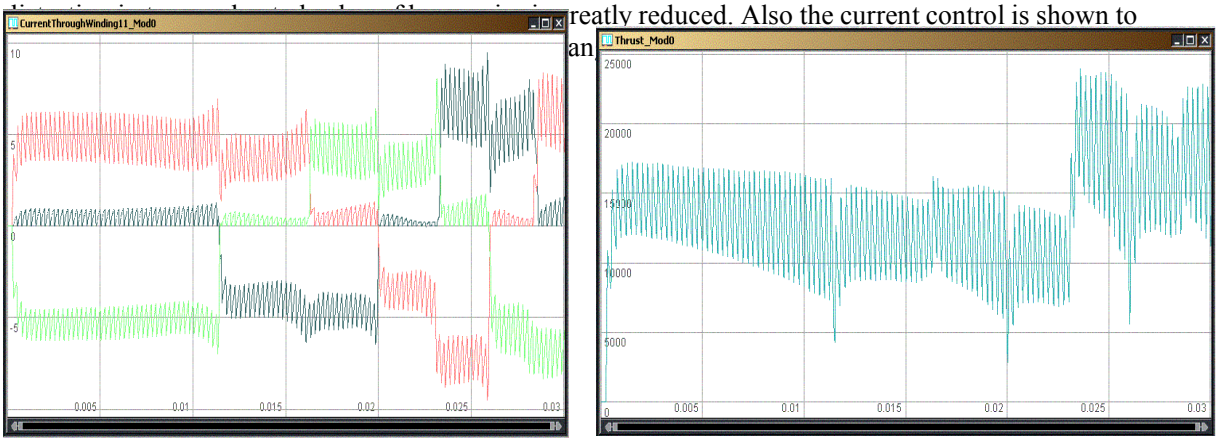

Fig. 20: 3-Phase currents and the torque for BLDC control

BLAC control

For BLAC, the value of $\varphi_q(v) = \left.\frac{d\lambda}{dv}\right|_q$ is found through Park transformation once the value of $\left.\frac{d\lambda}{dv}\right|_{a,b,c}$ is read from the Excel file. The current control is implemented using space vector modulation theory. Consider the following stator equations for $\alpha - \beta$ voltages,

$$v_{s\alpha} = R_S \cdot i_{s\alpha} + L_s \cdot \frac{di_{s\alpha}}{dt} - e_\alpha \tag{4}$$

$$v_{s\beta} = R_S \cdot i_{s\beta} + L_s \cdot \frac{di_{s\beta}}{dt} + e_\beta \tag{5}$$

Using Euler's first order approximation for current derivation, we get the following equation,

$$v_{s\alpha} = R_S \cdot i_{s\alpha} + L_s \cdot \frac{i_{s\alpha}(k+1) - i_{s\alpha}(k)}{T_s} - e_\alpha \tag{6}$$

$$v_{s\beta} = R_S \cdot i_{s\beta} + L_s \cdot \frac{i_{s\beta}(k+1) - i_{s\beta}(k)}{T_s} - e_\beta \tag{7}$$

By giving the value for the future current reference, $i_{s\alpha}(k+1)$, into the above equation, we can enforce the value for current time step $i_{s\alpha}(k)$ to be equal to $i_{s\alpha}(k+1)$ in the next time step.

The VTB schematic used to implement the BLAC control is shown below,

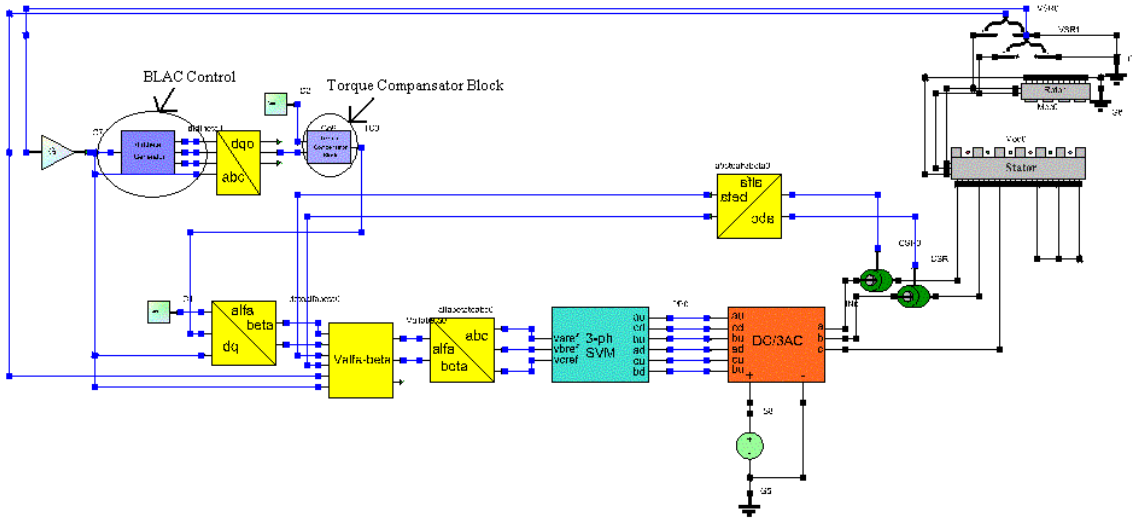

Fig. 21: The VTB schematic for BLAC control

The 3-phase currents and torque are shown below, and clearly the torque ripple is greatly reduced. The remaining noise in the torque waveform is due to the inverter switching. It shows a great improvement over the BLDC performance. Also the current control is shown to be effective since the 3 currents follow the change in reference current in just one time step.

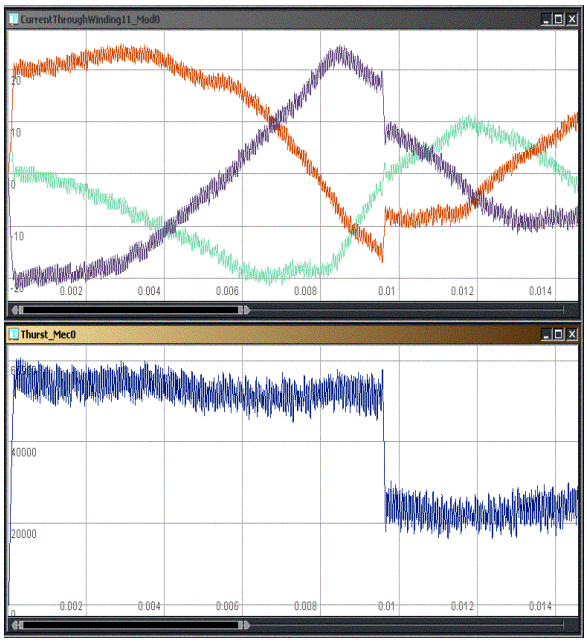

Fig. 22: 3-Phase Currents and the torque for BLAC control

Conclusion

This paper introduced the design of the hierarchical modular control for an electromagnetic aircraft launching system. Using the VTB simulation platform, different control strategies were compared. The modeling approach was also detailed, showing the capabilities of the new VTB version. The deadbeat current control, in conjunction with predictive algorithms, looks promising for high power application because of the possibility of limiting the sampling rate. But the problem of torque ripple arises due to BLDC type control of the motor and non-ideal back emf waveshape. A new method for torque ripple compensation was suggested and simulation results for BLAC and BLDC motors are reported. The results clearly demonstrate that BLAC is very efficient for fast current control and for torque ripple compensation.

References

[1]. R. Dougal, T. Lovett, A. Monti, E. Santi "A Multilanguage Environment for Interactive Simulation and Development of Controls for Power Electronics", IEEE Power Electronics Specialists Conference, Vancouver, Canada, June 17-22, 2001.

[2]. D. Patterson, A. Monti, R. Dougal, C. Brice, R. Pettus, D. Srinivas, K. Dilipchandra, T Bertoncelli, "Design and Simulation of an Electromagnetic Aircraft Launch System" *Record of the 37th Annual IEEE Industry Applications Society Conference, IAS 02,* Pittburgh, October 2002

[3]. A. Monti, M. Riva "How Predictive Algorithm can improve discrete-time variable structure control", IEEE PADI2, Piura (Peru')

[4]. A. Monti, K. Patel, D. Patterson, R. Dougal, "Modular Control for Electromagnetic Aircraft Launching System", PESC Conf. June 2003, Acapulco, Mexico

[5]. T. Lovett, A. Monti, R.A. Dougal, "The new architecture of the Virtual Test Bed", IEEE-COMPEL02, Mayaguez (Puerto Rico), June 2002

[6]. A. Monti, E. Santi, R. Dougal, M. Riva, "Rapid Prototyping of Digital Controls for Power Electronics", to appear on IEEE Trans. on Power Electronics, May 2003

[7]. P. Pillay, R. Krishnan "Application characteristics of permanent magnet synchronous and brushless DC motors for servo drives", Conf. Rec. IEEE/IAS Annu. Meeting, 1987, pp. 380-390

[8]. Carlson, M. Lajoie-Mazenc, J. Fagundes "Analysis of torque ripple due to phase commutation in brushless DC machines", IEEE Transactions on Industrial Application, vol. 28, No. 3, pp. 632-638, 1992.

[9]. C. Berendsen, G. Champenois, A. Bolopion "Commutation strategies for brushless DC motors: Influence on instant torque", IEEE Transactions on Power Electronics, vol. 8, no. 2, pp. 231-236, Apr. 1993.

[10]. S. Kang, S. Sul “Direct Torque Control of Brushless DC motor with nonideal trapezoidal back emf”, IEEE Transactions on Power Electronics, vol. 10, no. 6, pp. 796-802, Nov. 1995.

[11]. J. Holts, B. Beyer “Fast current trajectory tracking control based on synchronous optimal pulsewidth modulation”, IEEE Transactions on Industrial Applications, vol. 31, No. 5, pp. 1110-1120, Sept./Oct 1995.

[12]. J. Holts, L. Springob “Identification and compensation of torque ripple in high-precision permanent magnet motor drives”, IEEE Transactions on Industrial Applications, vol. 43, No. 2, pp. 309-320, April 1996.

[13]. A. Monti, M. Carpita, D. Colombo “A Generalised approach to torque ripple compensation in permanent magnet machine control”, ISIE 2000, Cholula, Puebla, Mexico.

[14]. D. Colombo, A. Monti, G. Secondo, “Comparing different approaches to electrical machine modeling: A brushless motor example”, IMACS99, Lisboa (Portugal), September 1999